Dependency of horizontal resolution and turbulent scheme on accumulation processes of low-level water vapor

Teruyuki KATO

Meteorological Research Institute, Tsukuba, Ibaraki, Japan (E-mail: tkato@mri-jma.go.jp)

1. Introduction

On 6 May, 2012, a supercell storm caused a strong tornado with Fujita scale 3 that struck Tsukuba City, located Kanto Plain in the middle part of Japan. The major formation factor of the supercell was the inflow of low-level humid air from the Pacific Ocean, as well as large temperature difference in the vertical (Kato 2013). In this study, the dependency of horizontal resolution and turbulent scheme on accumulation processes of low-level water over the ocean is examined using the Japan Meteorological Agency (JMA) nonhydrostatic model (Saito et al. 2007).

2. Experimental designs

Twelve-hour forecasts from 18 JST (=UTC+ 9hours) 05 May 2012 are conducted using initial and boundary conditions produced from 3-hourly available JMA mesoscale analyses with a horizontal resolution of 5 km. At first a 5km-resolution simulation with a large domain (2500x2000km) was conducted, and then the other simulations with a small domain (1000x600km) are conducted directly nested within large-domain forecasts. Horizontal resolutions of 5km, 2km, 1km and 500m are used, and 50 stretched layers (6 of which are set below a height of 500 m) are set in the vertical. A bulk-type microphysics parameterization scheme in which two moments are treated only for ice hydrometeors is used for precipitation processes, and the Kain- Fritsch convection parameterization scheme is additionally used only in 5km models. The turbulence closure scheme of Mellor-Yamada-Nakanishi-Niino level-3 (MYNN, Nakanishi and Niino 2006) is used in 5km, 2km, and 1km models, while Deardorff scheme (DD, 1980) is used in 1km and 500m models. Surface fluxes are calculated by a bulk method, in which the bulk coefficients are determined from the formula of Berjaars and Holtslag (1991) over both the sea and land.

3. Accumulation processes of low-level water vapor

In order to examine accumulation processes of low-level water, a budget analysis is made for water vapor amounts in vertical columns below a height of 936m (LWA). Local time difference of LWA is described as

$$\frac{\partial \mathrm{LWP}}{\partial t} = \mathrm{Conv_h} + \mathrm{Adv_v} + \mathrm{LH} + \mathrm{Others}, \quad (1)$$

where $\mathrm{Conv_h}$ is the horizontal convergence from lateral boundaries, $\mathrm{Adv_v}$ is the vertical transportation at upper panels of the vertical columns, LH is the latent heat flux from the surface, and Others denote the changes through condensation and evaporation. The last term is negligible because no cloud was found over the analysis domain.

An area with LWA ~ 8 mm on the left side of Fig. 1 at the initial (hereafter, called as target air column) moves east-northeastward, and after 12 hours the value of LWA increases by about 3 mm. A significant increase is found during the period when the air column crossed over a region with high sea surface temperature. A budget of the LWA in the target air column is examined.

The residual in the target air column calculated from $\mathrm{Conv_h}$ and $\mathrm{Adv_v}$ is considerably larger than the increase from LH, and total local change (RHS in Eq. (1)) is larger than the Lagrangian change directly calculated from LWA (Fig. 2a). This is caused by no consideration of horizontal advection ($\mathrm{Adv_h}$) as follows.

$$\frac{\mathrm{dLWP}}{\mathrm{dx}} = \frac{\partial \mathrm{LWP}}{\partial t} + \mathrm{Adv_h} \quad (2)$$

Here, $\mathrm{Adv_h}$ is estimated using winds at a height of 844m. Red lines in Fig. 2a show that the Lagrangian change calculated from Eqs. (1) and (2) almost agrees with the direct calculation from LWA, indicating the budget analysis is successful.

The kinematic change of LWA defined by the sum of $\mathrm{Conv_h}$, $\mathrm{Adv_v}$ and $\mathrm{Adv_h}$ is compared with the increase amount from LH (Fig. 2b). About two third of LWA increase (~ 2mm) is brought from the kinematic change, while the remaining is from LH. The increase over the ocean with high temperature is mainly from LH, while the kinematic change is dominant after 6 hour forecast.

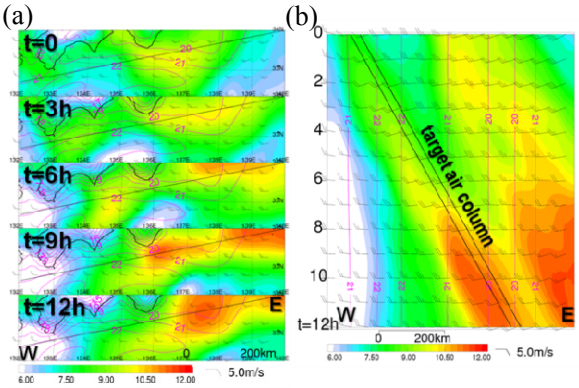

Fig. 1 (a) Distributions of 5km-model simulated LWA from the initial to 12 h forecast and (b) Hovmoller diagram across black lines in (a). Arrows show 936m- height horizontal winds, and pink contours show distributions of sea surface temperature.

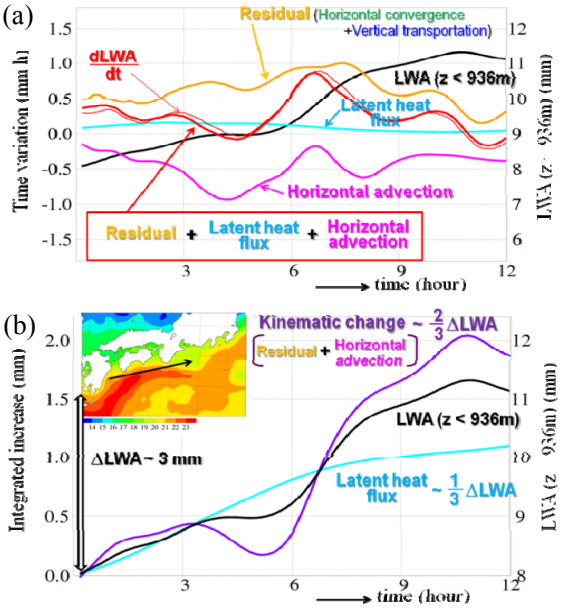

Fig. 2 (a) Time changes of 5km-model simulated LWA and its budgets for the target column shown in Fig. 1b and (b) those of integrated increases in kinematic change and latent heat flux. Thin red line in (a) shows the change directly calculated from LWA. Left-top panel in (b) shows the distribution of SST.

3. Dependency of horizontal resolution and turbulent scheme

Table 1 shows the contributions of kinematic change and LH on accumulation processes of low-level water for different horizontal resolutions and turbulent schemes of numerical models. The dependency on total increase is small; however, the contributions of kinematic change and LH are different for turbulent schemes. LH is smaller for DD, while the kinematic change is larger. It should be noted that the difference for horizontal resolution is remarkably smaller than that for turbulent schemes.

The above-mentioned differences are examined from water vapor amounts that are vertically transported by sub-grid and grid-resolved vertical motions (Fig. 3). Sub-grid transportation is almost limited below a height of 500m that is lower for DD. MYNN transports more water vapor upward than DD, which causes the difference in LH. Grid-resolved motions also transport more water vapor for MYNN, especially above a height of 500m, which reduces the accumulation amounts in the kinematic change.

Table 1 Total increases for the target air column, accumulated for 12 hours and their contents (kinematic change and latent heat flux).

	500m(DD)		1km(DD)	
Total (mm/12hours)	2.85	-	2.93	-
Kinematic change	2.11	74.3%	2.21	75.5%
Latent heat flux	0.73	25.7%	0.72	24.5%
5km(MYNN)		**2km(MYNN)**		**1km(MYNN)**
3.06	-	2.78	-	2.87	-
1.97	64.2%	1.71	61.4%	1.80	62.9%
1.10	35.8%	1.07	38.5%	1.06	37.1%

Last, vertical profiles of water vapor for the target air column are compared (Fig. 4). The increase of water vapor amounts near the surface for MYNN is almost a half for DD because of larger sub-grid transportation of water vapor. The difference between MYNN and DD is about 1 g/kg below a height of 400m. Meanwhile, water vapor is more accumulated for MYNN above a height of 500m. The difference for horizontal resolutions is also smaller than that for turbulent schemes. These results indicate that moist convection more easily forms using DD than using MYNN, although almost the same LWA is accumulated.

References

Beljaars, A.C.M. and A.A.M. Holtslag, 1991: *J. Appl. Meteor.*, **30**, 327-341.

Deardorff, J. W., 1980: *Bound.-Layer. Meteorol.*, **18**, 495-527.

Kato, 2013: *CAS/JSC Research Activities in Atmospheric and Oceanic Modeling*, **43**, 5.07-5.08.

Nakanishi, M. and H. Niino, 2006: *Bound.-Layer Meteor.*, **119**, 397- 407.

Saito, K., et al., 2007: *J. Meteor. Soc. Japan*, **85B**, 271-304.

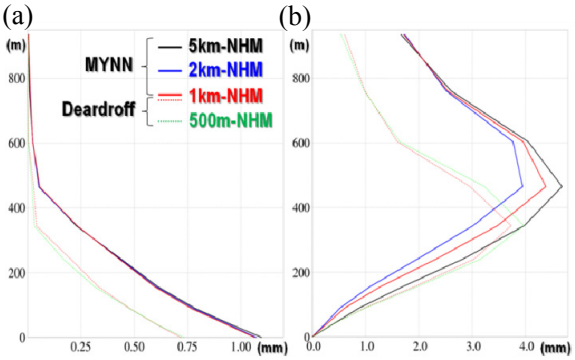

Fig.3 Vertical profiles of vertical transportation amounts of water vapor for the target air column, accumulated for 12 hours, by (a) sub-grid and (b) grid-resolved vertical motions.

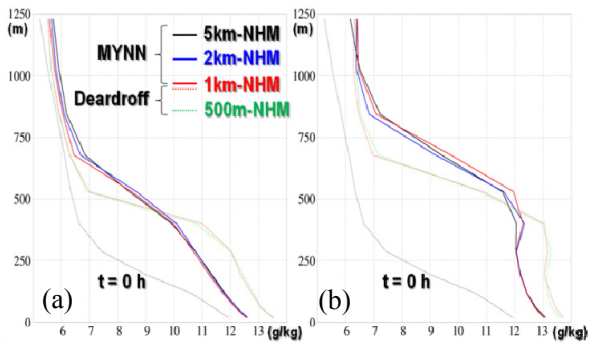

Fig. 4 Vertical profiles of water vapor for the target air column at (a) t = 6 hours and (b) t = 12 hours. The profile at the initial time is also drawn in each panel.